



Research  
Clean Energy—Review

## Flow-Induced Instabilities in Pump-Turbines in China

Zhigang Zuo, Shuhong Liu\*

*State Key Laboratory of Hydro Science and Engineering, Department of Thermal Engineering, Tsinghua University, Beijing 100084, China*

### ARTICLE INFO

*Article history:*

Received 17 April 2017

Revised 2 July 2017

Accepted 10 July 2017

Available online 3 August 2017

*Keywords:*

Pump-turbines

Flow-induced instability

Pressure fluctuations

S-shaped characteristics

Positive slopes

### ABSTRACT

The stability of pump-turbines is of great importance to the operation of pumped storage power (PSP) stations. Both hydraulic instabilities and operational instabilities have been reported in PSP stations in China. In order to provide a reference to the engineers and scientists working on pump-turbines, this paper summarizes the hydraulic instabilities and performance characteristics that promote the operational instabilities encountered in pump-turbine operations in China. Definitions, analytical methods, numerical and experimental studies, and main results are clarified. Precautions and countermeasures are also provided based on a literature review. The gaps between present studies and the need for engineering practice are pointed out.

© 2017 THE AUTHORS. Published by Elsevier LTD on behalf of the Chinese Academy of Engineering and Higher Education Press Limited Company. This is an open access article under the CC BY-NC-ND license (<http://creativecommons.org/licenses/by-nc-nd/4.0/>).

### 1. Introduction

Renewable-based electrical supply systems are intermittent by nature, and have a great impact on the stability and reliability of the electricity grid. Energy storage technologies are required as more renewables come online; of these technologies, hydropower pumped storage is the only commercially available grid-scale technology at present. In this technology, water is pumped to an upper reservoir if the energy supply is higher than the demand, and is then used to generate electricity when the demand is higher than the supply. In addition to load-leveling, this technology benefits the grid with grid frequency regulation and spinning reserves [1].

Although the earliest pumped storage power (PSP) stations were built in the Alpine region in the 1890s, the first PSP station in China appeared some 80 years later, in the form of small-scale mixed PSP stations in Gangnan and Miyun, with a total capacity of 11 MW and 22 MW, respectively [2]. Starting in the 1990s, the construction of large-scale PSP stations in China entered a period of fast development in response to the increasing demand caused by the high-speed development of the national economy. More and more PSP stations with a total capacity over 1000 MW are being constructed.

As the hydraulic components responsible for the energy trans-

formation between the generator/motor and water, reversible pump-turbines, which work in both turbine and pump modes, have replaced sets of separate turbines and pumps since the 1960s, due to their relatively compact sizes. Considering the flow directions at the inlet and outlet, pump-turbines can be categorized as axial flow, diagonal flow, or Francis pump-turbines, among others. Since Francis pump-turbines (henceforth referred to as pump-turbines for simplicity) have the widest range of working head, most modern designs fall into this category [3]. In order to reduce manufacturing and construction costs, and increase the unit hydraulic efficiencies, more pump-turbines are adopting a larger unit capacity and higher heads. Fig. 1 shows the unit capacity and head of pump-turbines in built PSP stations in China over time. Most unit capacities are now over 300 MW, and the highest head is over 600 m. The heads of several other PSP stations under construction or planning reach 600–700 m, such as those of Yangjiang, Jixi, Pingjiang, and Wulongshan.

Hydraulic instabilities such as pressure fluctuations are more severe with higher working heads, and may induce mechanical vibrations through fluid-structure interaction [4] and, in extreme cases, premature mechanical failures [5]. Certain flow characteristics such as vortices in the draft tube and turbine runner, and the rotor-stator

\* Corresponding author.

E-mail address: [liushuhong@mail.tsinghua.edu.cn](mailto:liushuhong@mail.tsinghua.edu.cn)

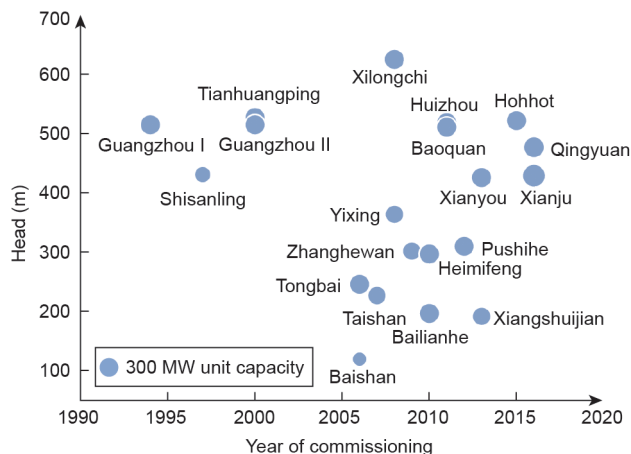


**Fig. 1.** Unit capacity and head of pump-turbines in built PSP stations in China over time. Unit capacities of pump-turbines are comparable to the areas of the circles.

interaction (RSI), are known for promoting large pressure fluctuations. It should also be noted that differences exist in the working head of pump-turbines between the turbine and pump modes, in order to account for the hydraulic losses in pipelines. The design of a pump-turbine first needs to guarantee the pump performance. Hence, pump-turbines share more similarity in shape with centrifugal pumps than with Francis turbines. Pump-turbines with higher heads, which correspond to lower values of specific speed ( $n_s$ ), that is,

$$n_s = \frac{3.65n\sqrt{Q}}{H^{3/4}} \quad (\text{m, } \text{m}^3 \cdot \text{s}^{-1}) \quad (1)$$

where  $n$ ,  $Q$ , and  $H$  are the runner rotating speed, the volumetric flow rate, and the hydraulic head, respectively, possess more prolonged flow channels. They are more prone to so-called S-shaped characteristics and positive slopes on performance curves in turbine and pump modes, respectively, which promote operational instabilities [6].

This paper systematically summarizes the hydraulic instabilities and performance characteristics that promote operational instabilities in pump-turbines in China, and illustrates the related flow mechanisms through a literature review. Precautions and countermeasures against these instabilities are also presented.

## 2. Hydraulic instabilities: Pressure fluctuations

Hydraulic instability problems have been reported in several PSP stations in China, along with their effects on the dynamic behavior of parameters, such as shaft line or head cover vibrations, shaft displacement, and operating difficulties. A schematic of the hydraulic components of a pump-turbine is shown in Fig. 2 [4] for reference.

### 2.1. Guangzhou I

The Guangzhou I PSP station has four pump-turbines, each with 300 MW unit capacity. The numbers of runner blades, guide vanes, and stay vanes are 7, 20, and 20, respectively.

During the first year of operation, it was reported that the pressure fluctuations in the vaneless space and the draft tube had high amplitudes when running at excessive partial load ( $\leq 40\%$  rated load) in turbine mode (Table 1) [7]. The main frequencies of pressure fluctuations in the vaneless space and the draft tube were the blade passing frequency (BPF)—which is equal to the number of runner blades times the runner rotational frequency—and near the rotational frequency, respectively. While in pump mode, the relative

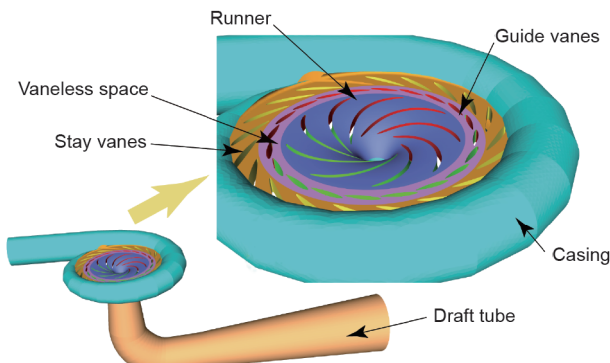


**Fig. 2.** Schematic of the hydraulic components of a pump-turbine. (Adapted from Ref. [4])

amplitude of pressure fluctuations in the vaneless space was in the range of 5%–6%. It reached 7.4% when  $H < 517$  m and  $Q > 59 \text{ m}^3 \cdot \text{s}^{-1}$ . In the startup of the pump mode, the amplitude of pressure fluctuations reached 51.6% [7]. According to Ref. [8], excessive throws (~800 μm) appeared in the upper and lower guide bearings in the No. 4 pump-turbine unit in the Guangzhou I PSP station, both in turbine mode and in pump mode, due to the uneven circumferential distribution of clearance in the bearings and to misalignment in the shaft system. It was also reported that in the first month after the commissioning of the Guangzhou I PSP station, 16 failures (out of 45) appeared in the startup, such as being unable to synchronize to the grid; some of these failures were caused by excessive pressure fluctuations [9].

### 2.2. Shisanling

The Shisanling PSP station has four pump-turbines, each with 200 MW unit capacity. The numbers of runner blades, guide vanes, and stay vanes are 7, 16, and 16, respectively.

Compared with the Guangzhou I PSP station, the pressure fluctuations in the vaneless space had higher amplitude at the Shisanling PSP station (Table 1 and Table 2) [7]. According to Ref. [7], preliminary research indicated that these pressure fluctuations were related to the combination of the numbers of runner blades and guide vanes. A larger vibration could be excited in the vaneless gap between 7 runner blades and 16 guide vanes. The throw of the turbine guide bearing was large since the commencement of the No. 1 unit in 1995, being 0.2 mm at the rated working condition, and reaching a maximum value of 0.38 mm. The high throw at different locations resulted in a large unit centrifugal inertia force and a stronger

**Table 1**  
Pressure fluctuations in the Guangzhou I PSP station (data from Ref. [7]).

		Relative amplitude of pressure fluctuations, $\Delta H/H$ (%)		
		Inlet of casing	Vaneless space	Draft tube
Turbine mode	Rated load	≤ 3.0	≤ 10.2	≤ 1.0
	Partial load	≤ 4.7	≤ 14.4	≤ 6.3
	Pump mode	≤ 1.8	≤ 5.8	≤ 1.0

**Table 2**  
Pressure fluctuations in the Shisanling PSP station (data from Ref. [7]).

		Relative amplitude of pressure fluctuations, $\Delta H/H$ (%)		
		Inlet of casing	Vaneless space	Draft tube
Turbine mode	Rated load	≤ 2.3	≤ 9.0	≤ 2.0
	Partial load	≤ 2.0	≤ 16.3	≤ 4.2
	Pump mode	≤ 2.4	≤ 11.6	≤ 1.8

structure vibration. The temperature of the guide bearing increased to a dangerous value due to the vibration. After adjustment of the bearing clearance, the throw of the turbine guide bearing was reduced to 0.14 mm at the rated condition, and to a maximum of 0.24 mm [10]. It was also reported that since the commencement of the station, synchronization failure (i.e., the unit cannot synchronize to the grid for more than 10 min after startup) occurred in every pump-turbine unit in the Shisanling PSP station every year [11].

### 2.3. Guangzhou II

The Guangzhou II PSP station has four pump-turbines, each with 300 MW unit capacity. The numbers of runner blades, guide vanes, and stay vanes are 7, 20, and 20, respectively.

**Table 3** [12] shows the vibration and the throw of the unit during field tests in 2001. The results show that the vibration of the upper guide bearing, lower guide bearing, and upper support frame was small in both turbine and pump modes, while the vibration of the turbine guide bearing and of the head cover was much larger. In turbine mode, the vibration velocity reached up to about  $12 \text{ mm}\cdot\text{s}^{-1}$  in the turbine guide bearing and up to about  $6 \text{ mm}\cdot\text{s}^{-1}$  in the head cover [12]. It was also reported that during 2002–2004, the pump-turbines experienced a number of abnormal shut-downs due to non-synchronization of the guide vanes [13].

### 2.4. Tianhuangping

The Tianhuangping PSP station has six pump-turbines, each with 300 MW unit capacity. The numbers of runner blades, guide vanes, and stay vanes are 9, 26, and 26, respectively.

As shown in **Table 4** [14], the pressure fluctuations in the vane-

less space were high in turbine mode (highest amplitude over 50%). **Table 5** [14] shows the vibrations and throws in the Tianhuangping PSP station.

During the test run of the first unit of the Tianhuangping PSP station, the throw of every guide bearing and the vibration of the frame in turbine mode were large, at  $H < 526 \text{ m}$  (designed head). The unit was unable to operate stably at the designed rotational speed of  $500 \text{ r}\cdot\text{min}^{-1}$ . Pressure fluctuations were also high in the vaneless space [15,16]. In April 2002, the occurrence of an abnormal noise was reported when the No. 1 unit of the Tianhuangping PSP station stopped from pump mode. It was believed that the late switch-off of the main brake and small opening (4%) of the guide vanes resulted in a zero flow rate in pump mode, which induced high-amplitude pressure fluctuations in the vaneless space [17]. On 4 January 2003, unit lifting due to upward thrust occurred during load increase in the No. 2 unit of the Tianhuangping PSP station. It stabilized after 10 min. Pressure in the upper labyrinth ring fluctuated up to 0.15 MPa, and the vibration of the head cover reached  $8.4 \text{ mm}\cdot\text{s}^{-1}$ . It was suspected that this may have been due to the large pressure fluctuations in the draft tube in the generating mode [18].

### 2.5. Yixing

The Yixing PSP station has four pump-turbines, each with 250 MW unit capacity. The numbers of runner blades, guide vanes, and stay vanes are 9, 26, and 26, respectively.

The pressure fluctuations in the Yixing PSP station are relatively lower than those in some other stations (**Table 6**) [19]. The relative amplitude in the vaneless space at 50% partial load in turbine mode is 4.2%. The maximum vibration of the head cover is  $0.82 \text{ mm}\cdot\text{s}^{-1}$ ,

**Table 3**

Vibrations and throws in the Guangzhou II PSP station (data from Ref. [12]).

Items		Value
Turbine mode	Vibration of the upper guide bearing, lower guide bearing, and upper support frame ( $\text{mm}\cdot\text{s}^{-1}$ )	< 0.9
	Vibration of turbine guide bearing ( $\text{mm}\cdot\text{s}^{-1}$ )	12.1–12.6
	Vibration of head cover ( $\text{mm}\cdot\text{s}^{-1}$ )	5.6–6.4
	Throw of upper and lower guide bearing shaft ( $\mu\text{m}$ )	17–70
	Throw of turbine guide bearing shaft ( $\mu\text{m}$ )	< 140
Pump mode	Vibration of the upper guide bearing, lower guide bearing, and upper support frame ( $\text{mm}\cdot\text{s}^{-1}$ )	< 1.2
	Vibration of turbine guide bearing ( $\text{mm}\cdot\text{s}^{-1}$ )	< 4.0
	Vibration of head cover ( $\text{mm}\cdot\text{s}^{-1}$ )	< 4.0
	Throw of upper and lower guide bearing shaft ( $\mu\text{m}$ )	20–85
	Throw of turbine guide bearing shaft ( $\mu\text{m}$ )	43–60

**Table 4**

Pressure fluctuations during off-design turbine conditions in the Tianhuangping PSP station (data from Ref. [14]).

Operation condition	P1	P2	P3	P4	P5	P6
$450 \text{ r}\cdot\text{min}^{-1}$	7.8%	3.9%	19.4%	15.60%	50.53%	23.32%
$475 \text{ r}\cdot\text{min}^{-1}$	5.8%	3.9%	19.4%	23.32%	54.40%	27.20%

P1, P2: between runner and bottom ring; P3, P4: between runner and head cover; P5, P6: vaneless space.

**Table 5**

Vibrations and throws in the Tianhuangping PSP station (data from Ref. [14]).

Operation condition	Head cover vibration ( $\text{mm}\cdot\text{s}^{-1}$ )	Throw of upper guide bearing ( $\mu\text{m}$ )	Throw of lower guide bearing ( $\mu\text{m}$ )	Throw of turbine guide bearing ( $\mu\text{m}$ )	Throw of thrust bearing ( $\mu\text{m}$ )
Turbine mode	4	135	251	> 500	160
Turbine mode no load	2.9–4			310–500	
Pumping phase modulation		160	120	62	163
Pump mode		102	61	398	45

and the throw of the turbine guide vanes is 71.18 μm [19].

An abnormal sound, as well as the non-synchronization of the guide vanes, occurred during the over-speed test of the No. 3 unit of the Yixing PSP station. It was shown that the pressure in the draft tube increased rapidly while the pressure in the spiral casing dropped, forming a negative water hammer, during the transition of the unit from reverse pump mode into turbine break condition. This problem was solved by reducing the closing speed of the guide vanes, according to Ref. [20]. Strong guide vane vibrations were experienced during the commissioning of pump starting, pump closing, and turbine mode in the over-speed and turbine trip tests of the No. 1 unit of the Yixing pump-turbine. This issue was corrected by making adjustments to the guide vane closing sequence (during turbine over-speed and turbine trip), or by opening the circuit breaker at a higher power (during pump closing) [21].

## 2.6. Xilongchi

The Xilongchi PSP station has four pump-turbines, each with 300 MW unit capacity. The numbers of runner blades, guide vanes, and stay vanes are 7, 20, and 20, respectively. The pressure fluctuations in the pump-turbines are shown in Table 7.

## 2.7. Baoquan

The Baoquan PSP station has four pump-turbines, each with 300 MW unit capacity. The numbers of runner blades, guide vanes, and stay vanes are 9, 20, and 20, respectively. The pressure fluctuations in the pump-turbines are shown in Table 8.

**Table 6**  
Pressure fluctuations in the Yixing PSP station (data from Ref. [19]).

		Relative amplitude of pressure fluctuations, ΔH/H (%)	
		Vaneless space	Draft tube wall
Turbine mode	Rated load	2.43	1.7
	50% partial load	4.2	3.4
Pump mode		1.3	0.4

**Table 7**  
Pressure fluctuations in the Xilongchi PSP station.

		Relative amplitude of pressure fluctuations, ΔH/H (%)	
		Vaneless space	Draft tube wall
Turbine mode	Rated load	4.8	0.8
	50% partial load	11.3	3.0
Pump mode		4.6	0.5

**Table 9**  
Throws and vibrations in the Baoquan PSP station.

		Synchronous guide vane opening		Non-synchronous guide vane opening	
Throws (μm)	Upper guide bearing	y direction	485.0	610.9	
	Lower guide bearing	x direction	436.7	492.6	
		y direction	513.3	603.2	
	Turbine guide bearing	x direction	213.3	269.3	
		y direction	277.4	277.5	
Vibrations (mm·s <sup>-1</sup> )	Upper support frame	x direction	44.3	52.4	
		y direction	42.2	50.4	
	Lower support frame	x direction	54.7	54.7	
		y direction	45.2	54.6	
		z direction	28.5	34.4	

As shown in Table 9, with non-synchronous guide vanes opening using misaligned guide vanes (MGVs), the flow in the vaneless space became non-uniform in different guide vane channels, increasing the vibrations and throws of the unit.

## 2.8. Huizhou

The Huizhou PSP station has eight pump-turbines, each with 300 MW unit capacity. The numbers of runner blades, guide vanes, and stay vanes are 9, 20, and 20, respectively. Pressure fluctuations, throws and vibrations in the Huizhou PSP station are listed in Table 10 and Table 11.

The vibrations of the unit exceeded the limit under the conditions of rated speed and no load, due to the unsynchronized opening of the guide vanes. Using MGVs induced especially large vibrations of the servomotor, resulting in fractures in the connecting bolts of the servomotor in the unit test. Improvement was made by adding two extra MGVs to reduce the stress on a single vane [22].

## 2.9. Summary

With the data collection above, it can be seen that the pressure fluctuations in the vaneless space between the runner blades and the guide vanes have the maximum amplitudes in pump-turbines. It has been established that these characteristics of pressure fluctuations are promoted by the effect of RSI, including the potential flow (inviscid) interaction and the wake (viscous) interaction [4].

Tanaka [23] proposed a model to explain the diametrical vibration modes in high-head pump-turbines induced by RSI. When the runner blades pass across the wakes of the vanes, the flow interference induces vibrations/pressure fluctuations in the runner with frequencies of  $n \cdot Z_g f_n$  when observed from the rotating coordinates, and with frequencies of  $m \cdot Z_r f_n$  (where  $Z_r f_n$  is the BPF) when observed from stationary coordinates, where  $Z_g$  is the number of guide vanes,  $Z_r$  is the number of runner blades,  $f_n$  is the rotational frequency of the runner, and  $m$  and  $n$  are arbitrary integers. The vibration mode with  $k$  diametrical nodes is calculated by the equation  $n \cdot Z_g \pm k = m \cdot Z_r$ . An example of RSI with  $Z_g = 20$  and  $Z_r = 6$  is shown in Fig. 3 [23], which includes a schematic of the phase lag of the interferences and the different vibration modes in terms of the number of diametrical nodes.

**Table 8**  
Pressure fluctuations in the Baoquan PSP station.

		Relative amplitude of pressure fluctuations in vaneless space, ΔH/H (%)	
Turbine mode	Rated load	3.42	
	50% partial load	9.52	
Pump mode		2.07	

**Table 10**

Pressure fluctuations in the Huizhou PSP station.

Turbine mode	Relative amplitude of pressure fluctuations, $\Delta H/H$ (%)	
	Vaneless space	Draft tube wall
Rated load	4.8	0.8
Partial load	5.0	3.0
Pump mode	3.6	

**Table 11**

Throws and vibrations in the Huizhou PSP station.

Throws ( $\mu\text{m}$ )	Upper guide bearing	Peak value	
		x direction	y direction
Vibrations ( $\text{mm}\cdot\text{s}^{-1}$ )	Upper support frame	253	269
		284	275
Vibrations ( $\text{mm}\cdot\text{s}^{-1}$ )	Turbine guide bearing	273	232
		1.0	1.1
Vibrations ( $\text{mm}\cdot\text{s}^{-1}$ )	Lower support frame	0.6	0.9
		3.1	8.0

Hydraulic impacts due to interference between runner blades and guide vanes

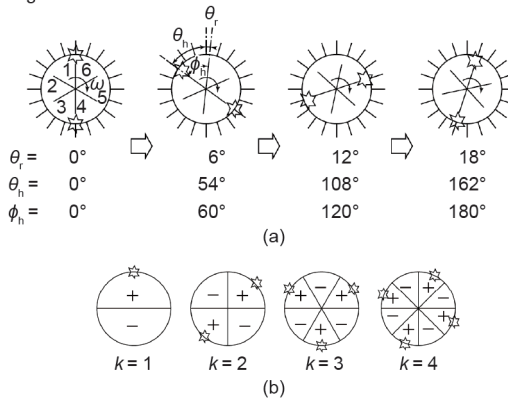


Fig. 3. Vibrations in the vaneless space due to RSI in the pump-turbine [23]. (a) Hydraulic interference between runner blades and guide vanes; (b) vibration modes with  $k$  diametrical nodes.

Ref. [4] summarizes the major parameters of pump-turbines that influence pressure fluctuations. Pump-turbines working under off-design conditions have pressure fluctuations of larger amplitudes, due to the flow separations in the runner/guide vane channels. It is also reasonable that the distance of the vaneless gap is another determinant of the pressure fluctuations. An optimum distance of the vaneless gap exists, in terms of the lowest amplitude of pressure fluctuations in pump mode, according to Ref. [24]. Another study showed that a smaller vaneless gap caused higher pressure fluctuations in the vaneless gap in pump mode, and lower pressure fluctuations in turbine mode [25]. Regarding the cavitation condition, Ref. [24] reported an increase of 30%–40% in the amplitude of the pressure fluctuations at the critical cavitation coefficient number, compared with the non-cavitating operating points. By experimentally comparing three different pump-turbine models, it was shown that after increasing the guide vanes' height by 40%, the amplitude of the pressure fluctuations in the vaneless space was reduced by 20%–30%, whereas the thickness of the guide vanes had

little influence on pressure fluctuations [26]. Research also showed that the application of twisted runner blades helped to reduce the pressure fluctuations [27].

### 3. Performance characteristics promoting operational instabilities: S-shaped characteristics and positive slopes

In a pumping system, two types of instability can be described, in terms of the transient response to an initial perturbation: static instabilities, which refer to a continuous increase in the amplitude of the perturbation; and dynamic instabilities, which refer to oscillation of the continually increasing amplitude of the perturbation [28]. The static instability of the system is associated with a divergence from the initial operating point, and can be characterized by the (quasi-)steady-state performance characteristics. Static stability is a necessary but insufficient condition for dynamic stability. Although this criterion is less rigorous than the dynamic instability, it provides a more practical standard to distinguish between instabilities in engineering applications.

Indeed, by ignoring the pipeline characteristics, the two performance characteristics of pump-turbines that promote operational instabilities, that is, the S-shaped characteristics in turbine mode and the positive slopes in pump mode, can be readily derived by the static stability criterion described above. The S-shaped characteristics in  $Q_{ED} \sim n_{ED}$  curves are shown in Fig. 4(a), in which  $Q_{ED} = Q/(D^2\sqrt{E})$  denotes the discharge factor,  $n_{ED} = nD/\sqrt{E}$  denotes the speed factor, and  $T_{ED} = T/(\rho D^3 E)$  denotes the torque factor (where  $E$  is the specific hydraulic energy of the unit and  $T$  is the torque) [29]. Characteristic curves in terms of unit flow rate and speed,  $Q_{11} \sim n_{11}$ , are also seen in the literature [6]. In pump mode, the slope of the  $E_{nD} \sim Q_{nD}$  characteristic can be positive in a limited range of discharge (Fig. 4(b)) [29], in which  $E_{nD} = E/(n^2 D^2)$  denotes the energy coefficient, and  $Q_{nD} = Q/(nD^3)$

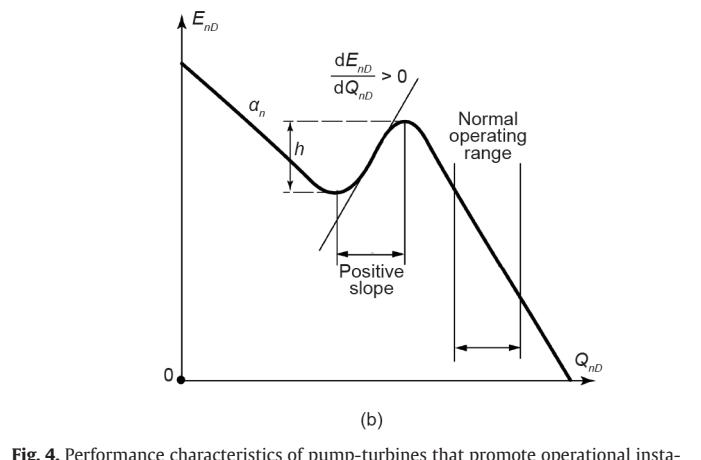
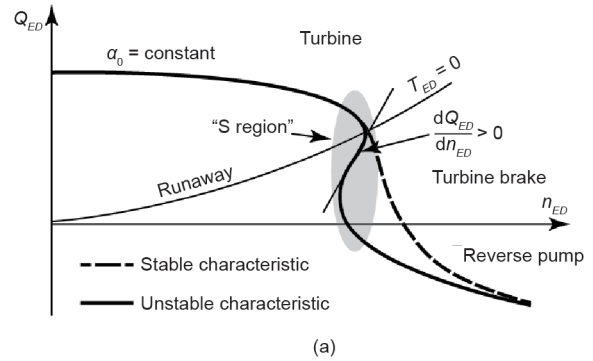


Fig. 4. Performance characteristics of pump-turbines that promote operational instabilities. (a) S-shaped characteristics; (b) positive slope. (Adapted from Ref. [29])

denotes the discharge coefficient. Characteristic curves in terms of hydraulic head and flow rate,  $H \sim Q$ , are also seen in the literature.

Simply speaking, the loss of the one-to-one correspondence of the horizontal and vertical coordinates in the so-called unstable zones of the S-shaped characteristics and the positive slopes, as shown in Fig. 4, promotes unstable oscillations of the operating conditions during certain transient processes. In fact, the S-shaped characteristics will promote difficulties in synchronizing with the power grid in turbine startups, unstable performance in turbine load rejections, and so forth, as schematically shown in Fig. 5(a) [6], where  $Q_{11} = Q/(D^2\sqrt{H})$  is the unit flow rate,  $n_{11} = nD/\sqrt{H}$  is the unit speed, and  $T_{11} = T/(\rho D^3 H)$  is the unit torque. For example, You et al. [30] reported these instabilities during trial operations at the Tianhuangping power station under a low water head. Fig. 5(b) [3] illustrates an extreme case during pump startup, where the pipeline characteristics pass through the positive slope zones at the guide vane opening from 40% to 50%. Instead of passing from A → B → C → D → F, as the operation is intended to proceed, it may pass through A → B → C → D → E, because of the existence of the positive slopes.

A detailed discussion of the flow mechanism of the S-shaped characteristics can be found in Ref. [6]. Through experimental and computation fluid dynamics studies, complex flow features in the region of S-shaped characteristics in the pump-turbines, such as, backflow at the runner inlet, stationary vortex formation, and rotating stall in the vaneless space, have been identified, especially under speed no-load conditions. Similarly, secondary flows [31], rotating stall in vaneless space and guide vane channels [32–46], and impeller inlet pre-rotation [34] are believed to form the main flow mechanism of the positive slopes.

Considering the instabilities promoted by these two performance characteristics, safety margins are usually contractually prescribed for the designers. Fig. 6(a) [6] illustrates the derivation of the safety margin for the S-shaped characteristics. First, model tests are conducted with increments of guide vane openings of no more than 1°.

The slope of the  $Q_{11} \sim n_{11}$  curves, with constant guide vane opening at the intersections with the runaway curve, increases with increasing guide vane opening. A critical point is defined at which  $Q_{11}/n_{11} \sim 0$ , or  $T_{11}/n_{11} \sim 0$  on  $T_{11} \sim n_{11}$  curves [47,48]. The safety margin on the head is then calculated as the difference between the head at the critical point and at the unit minimum head within the allowable frequency range of the power grid (50.5 Hz in Fig. 6(a)). Minimum values of this margin have been suggested for engineering practice (40 m in Ref. [48] and 20 m in Ref. [49]). Regarding the safety margin for the positive slopes, although positive slopes can exist on multiple pump performance curves with constant guide vane openings, the pump performance curve at the highest pump head is typically considered to assess the safety margin. The pump performance curve and the equivalent pipeline characteristics in the operational head range of the pump-turbine are shown in Fig. 6(b) [50], in the case where the frequency of the power grid oscillates in the range of  $(f - \Delta f_1, f + \Delta f_2)$  [50]. The safety margin on the head is specified as the ratio against the maximum working head  $H_{sm}/H_{max}$ . Ref. [51] suggests a value of no less than 2% in China, corresponding to a 49.8–50.5 Hz power grid frequency oscillation range. Different values have been assigned in model acceptance tests with different PSP stations in China, such as 3% for Baoquan [52] and Xiangshuijian [53], and 4% for Heimifeng [54].

It is shown that the design of the pump-turbine runner has a great influence on the performance characteristics. For example, a parametric study showed that regarding turbine performance, in order to make a pump-turbine more stable, one should increase the radius of curvature on the pressure side of the leading edge in turbine mode, decrease the inlet radius, increase the inlet blade angle, or increase the length of the blade [55]. By investigating three model pump-turbines with different guide vane heights and runner vane thicknesses, it was discovered that when the runner vane thickness was increased by 5%, decreases of 5% were achieved in the corresponding discharges of the “saddle” peak, and the best efficiency

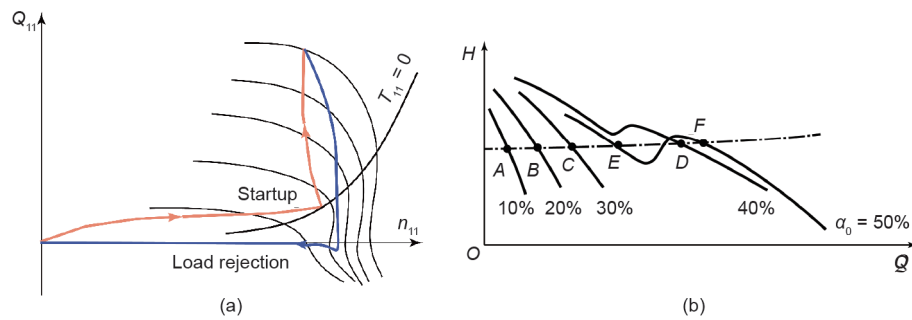


**Fig. 5.** Operational instabilities in the transient processes of pump-turbines. (a) Turbine startup and load rejection [6]; (b) pump startup (adapted from Ref. [3]).

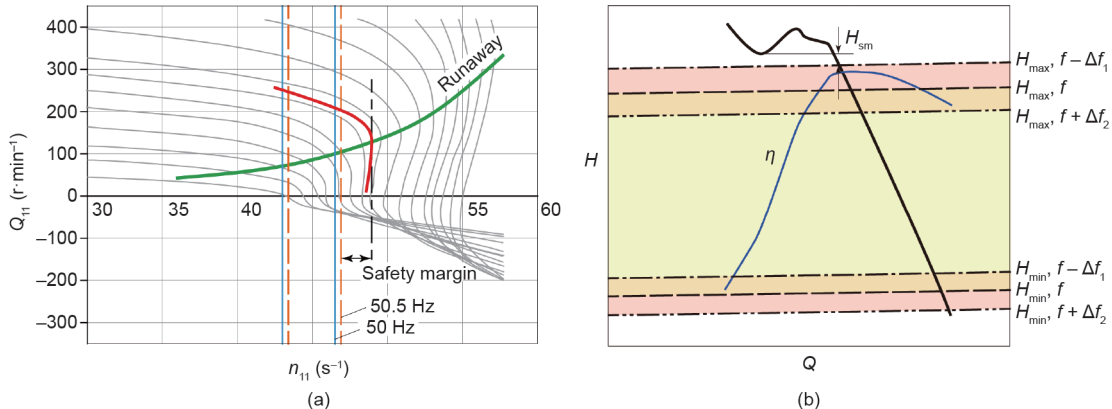


**Fig. 6.** Safety margins of pump-turbines. (a) S-shaped characteristics [6]; (b) positive slope (adapted from Ref. [50]).

point on the  $H \sim Q$  curve was achieved [26].

In dealing with the difficulties in synchronization with the power grid promoted by the S-shaped characteristics, it should be noted that a technique applying MGVs has been adopted in a number of PSP stations. This technique was first introduced on COO II (Belgium) pump-turbines [56], and has been applied in the Tianhuangping [57] and Yixing [58] PSP stations in China. A large number of research studies have been carried out on the flow mechanism, the influence on the pressure fluctuations, and the optimization of the application of MGVs. Readers are encouraged to refer to Ref. [6] for details.

## 4. Conclusions

Pump-turbines with higher head and larger capacity are more prone to hydraulic instabilities, such as pressure fluctuations, and to performance characteristics that promote operational instabilities, such as S-shaped characteristics and positive slopes in turbine and pump modes, respectively. This paper summarizes the hydraulic instabilities encountered in pump-turbine operations in PSP stations in China. The most detrimental pressure fluctuations in pump-turbines, that is, pressure fluctuations in the vaneless space, have been identified. An analytical method of the major frequencies that considers the main flow mechanism has been presented. Along with a description of pump-turbine operations in China, an introduction to unstable performance characteristics has been provided, which included the instability criterion, definitions, induced instabilities during transient processes, the flow mechanism, precautions, and means of countering such issues.

## Acknowledgements

The authors would like to thank the National Natural Science Foundation of China (51476083) for its financial support.

## Compliance with ethics guidelines

Zhigang Zuo and Shuhong Liu declare that they have no conflict of interest or financial conflicts to disclose.

## Nomenclature

$D$	Diameter of runner
$E$	Specific hydraulic energy
$E_{nD}$	Energy coefficient, $E_{nD} = E/(n^2 D^2)$
$f_n$	Rotational frequency of the runner
$H$	Hydraulic head
$H_{sm}$	Safety margin on head
$k$	Number of diametrical nodes
$m$	Arbitrary integer
$n$	Runner rotating speed, arbitrary integer
$n_{11}$	Unit speed, $n_{11} = nD/\sqrt{H}$
$n_{ED}$	Speed factor, $n_{ED} = nD/\sqrt{E}$
$n_s$	Specific speed, $n_s = \frac{3.65n\sqrt{Q}}{H^{3/4}}$ (m, $\text{m}^3 \cdot \text{s}^{-1}$ )
$Q$	Volumetric flow rate
$Q_{11}$	Unit flow rate, $Q_{11} = Q/(D^2 \sqrt{H})$
$Q_{ED}$	Discharge factor, $Q_{ED} = Q/(D^2 \sqrt{E})$
$Q_{nD}$	Discharge coefficient, $Q_{nD} = Q/(nD^3)$
$T$	Torque
$T_{11}$	Unit torque, $T_{11} = T/(\rho D^3 H)$
$T_{ED}$	Torque factor, $T_{ED} = T/(\rho D^3 E)$
$Z_g$	Number of guide vanes
$Z_r$	Number of runner blades
$\Delta H$	Amplitude of pressure fluctuations

## References

- [1] Rau NS. The state of energy storage in electric utility systems and its effect on renewable energy resources. Washington, DC: US Department of Energy; 1994 Aug. Report No.: NREL/TP-462-5337. Contract No.: AC36-83CH10093.
- [2] Zhang N, Dong HH, He XM. Constructions of pumped storage power stations in China. China Three Gorges 2010;(6):12–5. Chinese.
- [3] Mei ZY. Technology of pumped storage power generation. Beijing: China Machine Press; 2000. Chinese.
- [4] Zuo ZG, Liu SH, Sun YK, Wu YL. Pressure fluctuations in the vaneless space of high-head pump-turbines—A review. Renew Sust Energ Rev 2015;41:965–74.
- [5] Egusquiza E, Valero C, Huang XX, Jou E, Guardo A, Rodriguez C. Failure investigation of a large pump-turbine runner. Eng Fail Anal 2012;23:27–34.
- [6] Zuo ZG, Fan HG, Liu SH, Wu YL. S-shaped characteristics on the performance curves of pump-turbines in turbine mode—A review. Renew Sust Energ Rev 2016;60:836–51.
- [7] Wu MY. Analysis and comparison of the pump-turbine performance between Guangzhou and Shisanling pumped storage power stations. Dongfang Electr Mach 1995;(3):66–72. Chinese.
- [8] Liao JK. Solution of excessive vibrations and throws in a pump-turbine. Yunnan Water Power 2007;23(5):91–3,105. Chinese.
- [9] Wei BZ. Selection of electromechanical devices in Guangzhou pumped storage power stations. Water Power 1993;(7):73–5. Chinese.
- [10] Wang ZG, Liu JW. Analysis and treatment of abnormal axis and throw of a pumped storage unit. Mech Electr Tech Hydropower Stat 2003;26(3):52–5. Chinese.
- [11] Xu QF. Synchronization failure analysis for Shisanling pumped storage power station and the solutions. Hydropower Autom Dam Monit 2007;31(3):27–30. Chinese.
- [12] Wei BZ. Vibration evaluation of pumped-storage generating unit of Guangzhou pumped storage plant (second stage). Hydro Power 2001;(11):48–51. Chinese.
- [13] Zhong XH. Modifications of the monitoring system of the guide vane openings in Guangzhou pumped storage power station B. Mech Electr Tech Hydropower Stat 2007;30(1):45–7. Chinese.
- [14] He SR. Analysis of vibration in Tianhuangping I pumped storage power station. Mech Electr Tech Hydropower Stat 1999;(1):1–9. Chinese.
- [15] Sun JM, Zhu YX, Han ZX. Improvement of no-load stability of No. 1 pump-turbine under the condition of low head area in Tianhuangping pumped-storage power plant. Hydro Power 2001;(6):60–3. Chinese.
- [16] He SR. The apply of MGV device in Tianhuangping pumped-storage power station. J Hydroelectr Eng 2002;(3):88–100. Chinese.
- [17] Kong LH. Analysis of abnormal sounds in working condition change-over for high-head pump-turbine. Mech Electr Tech Hydropower Stat 2004;27(6):12–4. Chinese.
- [18] Le ZC, Kong LH. Cause analysis on rotating part lifting of Unit 2 in Tianhuangping pumped storage plant. Mech Electr Tech Hydropower Stat 2005;28(5):11–3. Chinese.
- [19] Yan L, Li CJ. Design of the pump-turbine and the auxiliary device in Yixing pumped storage power station. In: Proceedings of the engineering construction of pumped storage power stations (2009). Beijing: China Electric Power Press; 2009. Chinese.
- [20] Cai J, Zhou XJ, Deng L, Zhang WH. The research of the abnormal water hammer phenomenon based on the Unit 3 over speed test of Jiangsu Yixing pumped storage power station. Hydro Power 2009;35(2):76–9. Chinese.
- [21] Nennemann B, Parkinson É. Yixing pump turbine guide vane vibrations: Problem resolution with advanced CFD analysis. In: Proceedings of the 25th IAHR Symposium on Hydraulic Machinery and Systems; 2010 Sep 20–24; Timișoara, Romania. Bristol: IOP Publishing, Ltd.; 2010. p. 012057.
- [22] Hu NN, Dong C. Vibration effect of opening guide vanes desynchronized on pumped storage units. Hydropower Autom Dam Monit 2011;35(6):40–3. Chinese.
- [23] Tanaka H. Vibration behaviour and dynamic stress of runners of very high head reversible pump-turbines. In: Pejovic S, editor Proceedings of the 15th IAHR Symposium on Hydraulic Machinery and Cavitation; 1990 Sep 11–14; Belgrade, Yugoslavia; 1990.
- [24] Liu JS, Guan RQ. Experimental study of pressure fluctuations in Francis pump turbines. Report. Beijing: Tsinghua University; 1983. Report No.: TH83021. Chinese.
- [25] Sun YK, Zuo ZG, Liu SH, Wu YL, Liu JT. Numerical simulation of the influence of distributor pitch diameter on performance and pressure fluctuations in a pump-turbine. In: Wu Y, Wang Z, Liu S, Yuan S, Luo X, Wang F, editors IOP Conference Series: Earth and Environmental Science, Volume 15: The 26th IAHR Symposium on Hydraulic Machinery and Systems; 2012 Aug 19–23; Beijing, China. Bristol: IOP Publishing, Ltd.; 2012. p. 072037.
- [26] Kawamoto K, Niikura K, Satoh J, Harada T, Terasaki A. Reduction of stress amplitude in the runner of ultrahigh head pump turbines. Trans Jpn Soc Mech Eng B 1993;59(558):481–6. Japanese.
- [27] Ran HJ, Luo XW, Zhang Y, Zhuang BT, Xu HY. Numerical simulation of the unsteady flow in a high-head pump turbine and the runner improvement. In: Proceedings of ASME 2008 Fluids Engineering Division Summer Meeting Collocated with the Heat Transfer, Energy Sustainability, and 3rd Energy Nanotechnology Conferences; 2008 Aug 10–14; Jacksonville, FL, USA. New York: American Society of Mechanical Engineers; 2008. p. 1115–23.
- [28] Greitzer EM. The stability of pumping systems—The 1980 Freeman Scholar lec-

- ture. *J Fluids Eng* 1981;103(2):193–242.
- [29] International Electrotechnical Commission. IEC 60193 Hydraulic turbines, storage pumps and pump-turbines—Model acceptance tests. Geneva: International Electrotechnical Commission; 1999.
- [30] You GH, Kong LH, Liu DY. Pump-turbine S zone & its effect at Tianhuangping pumped storage power plant. *J Hydraul Eng* 2006;25(6):136–9. Chinese.
- [31] Braun O, Kueny JL, Avellan F. Numerical analysis of flow phenomena related to the unstable energy-discharge characteristic of a pump-turbine in pump mode. In: Proceedings of ASME 2005 Fluids Engineering Division Summer Meeting; 2005 Jun 19–23; Houston, TX, USA. New York: American Society of Mechanical Engineers; 2005. p. 1075–80.
- [32] Kubota T, Kushimoto S. Visual observation of internal flow through high-head pump-turbine. *Fuji Electric Rev* 1980;26(4):133–44.
- [33] Stepanik HE, Brekke H. Unsteady flow phenomena in a reversible Francis pump turbine. In: Rohatgi US, editor. Fluid Machinery Forum—1990; 1990 Jun 4–7; Toronto, ON, Canada. New York: American Society of Mechanical Engineers; 1990. p. 9–14.
- [34] Eisele K, Muggli F, Zhang Z, Casey M, Sallaberger M, Sebestyen A. Experimental and numerical studies of flow instabilities in pump-turbine stages. In: Brekke H, Duan CG, Fisher RK, Schilling R, Tan SK, Winoto SH, editors. Hydraulic machinery and cavitation: Proceedings of the XIX IAHR Symposium; 1998 Sep 9–11; Singapore. Singapore: World Scientific Publishing Co. Pte. Ltd.; 1998. p. 168–75.
- [35] Braun O. Part load flow in radial centrifugal pumps [dissertation]. Lausanne: École Polytechnique Fédérale de Lausanne; 2009.
- [36] Pacot O. Large scale computation of the rotating stall in a pump-turbine using an overset finite element large eddy simulation numerical code [dissertation]. Lausanne: École Polytechnique Fédérale de Lausanne; 2014.
- [37] Pacot O, Kato C, Guo Y, Yamada Y, Avellan F. Large eddy simulation of the rotating stall in a pump-turbine operated in pumping mode at a part-load condition. *J Fluids Eng* 2016;138(11):111102.
- [38] Yang J, Pavesi G, Yuan S, Cavazzini G, Ardizzon G. Experimental characterization of a pump-turbine in pump mode at hump instability region. *J Fluids Eng* 2015;137(5):051109.
- [39] Pavesi G, Cavazzini G, Yang J, Ardizzon G. Flow phenomena related to the unstable energy-discharge characteristic of a pump-turbine in pump mode. In: Proceedings of the 15th International Symposium on Transport Phenomena and Dynamics of Rotating Machinery (ISROMAC-15); 2014 Feb 24–28; Honolulu, HI, USA; 2014.
- [40] Pavesi G, Yang J, Cavazzini G, Ardizzon G. Experimental analysis of instability phenomena in a high-head reversible pump-turbine at large partial flow condition. In: Proceedings of the 11th European Conference on Turbomachinery Fluid Dynamics and Thermodynamics; 2015 Mar 23–27; Madrid, Spain; 2015. p. ETC2015-060.
- [41] Pavesi G, Cavazzini G, Ardizzon G. Numerical analysis of the transient behaviour of a variable speed pump-turbine during a pumping power reduction scenario. *Energies* 2016;9(7):534.
- [42] Li W, Pan ZY, Shi WD. Numerical investigation of pump-turbines with different blades at pump conditions. *J Adv Manuf Syst* 2012;11(2):143–50.
- [43] Xia LS, Cheng YG, Zhang XX, Yang JD. Numerical analysis of rotating stall instabilities of a pump-turbine in turbine mode. In: Désy N, Deschênes C, Guibault F, Page M, Turgeon M, Giroux AM, editors. IOP conference series: Earth and environmental science, volume 22: The 27th IAHR Symposium on Hydraulic Machinery and Systems; 2014 Sep 22–26; Montreal, QC, Canada. Bristol: IOP Publishing, Ltd.; 2014. p. 032020.
- [44] Yin JL, Liu JT, Wang LQ, Jiao L, Wu DZ, Qin DQ. Performance prediction and flow analysis in the vaned distributor of a pump turbine under low flow rate in pump mode. *Sci China Tech Sci* 2010;53(12):3302–9.
- [45] Li DY, Wang HJ, Xiang GM, Gong RZ, Wei XZ, Liu ZS. Unsteady simulation and analysis for hump characteristics of a pump turbine model. *Renew Energ* 2015;77:32–42.
- [46] Li DY, Gong RZ, Wang HJ, Wei XZ, Liu ZS, Qin DQ. Numerical investigation on transient flow of a high head low specific speed pump-turbine in pump mode. *J Renew Sustain Energy* 2015;7(6):063111.
- [47] Chen SY, Qiu SP, Fang J. Key points in compilations of technical conditions in turbine model tests. *East China Eng Techn* 2013;34(3):1–4. Chinese.
- [48] Chen SY, Li CJ, Zhou J, Shen JC, Qiu SP, Zheng YX. Prognosis on the stability of pump-turbine and the countermeasures. *Water Power* 2011;37(12):50–4. Chinese.
- [49] Yu JX, Li JW, Chen L, Ren SC, Jiang ML, Li HL. Discussions on main hydraulic performance parameters' model acceptance test of mixed flow pump turbine. *Mech Electr Tech Hydropower Stat* 2012;35(6):1–7. Chinese.
- [50] Qin DQ, Zhang LF. The proposal for the hump safety margin at pump maximum head of pump turbine. *Large Electr Mach Hydraul Turb* 2006;(4):46–8. Chinese.
- [51] General Administration of Quality Supervision, Inspection and Quarantine of the People's Republic of China, Standardization Administration of the People's Republic of China. GB/T 22581-2008 Fundamental technical requirements for Francis pump-turbine. Beijing: Standards Press of China; 2009. Chinese.
- [52] Wang SJ, Hu QJ. Model acceptance test of pump-turbine for the Baoquan pumped storage power station. In: Proceedings of the engineering construction of pumped storage power stations (2006). Beijing: China Electric Power Press; 2006. p. 59–62. Chinese.
- [53] Li H, Xu JX, Zhao YN. Model acceptance test for the pump turbine of Xiangshui-jian pumped storage unit in Lausanne, Switzerland. *Large Electr Mach Hydraul Turb* 2011;(3):50–3,57. Chinese.
- [54] Zheng JX, Zhang JZ, Zeng ZX, Zeng WC, Yu JX, Ren SC. Model acceptance test and performance analysis of pump-turbine of Heimifeng pumped-storage power station. *Water Power* 2010;36(7):63–5. Chinese.
- [55] Olimstad G, Nielsen T, Børresen B. Dependency on runner geometry for reversible-pump turbine characteristics in turbine mode of operation. *J Fluids Eng* 2012;134(12):121102.
- [56] Klemm D. Stabilisierung der kennlinien einer pumpenturbine im bereich zwischen turbinen-teillast und rückwärtspumpenbetrieb. *Voith Forschung und Konstruktion* 1982;28(2):2.1–7. German.
- [57] Ma MG. Analysis of failure in paralleling operation at low head of a pump-turbine unit and its solution. *Electromech Tech Hydropower Stat* 2002;(2):37–9. Chinese.
- [58] Li HB. Application of MGV in pumped storage power plant. *Mech Electr Tech Hydropower Stat* 2008;31(1):15–6,33. Chinese.